journal

J. Am. Ceram. Soc., 79 [8] 2091–97 (1996)

Rare-Earth Melilite Solid Solution and Its Phase Relations with Neighboring Phases

Zhen-Kun Huang and I-Wei Chen*

Materials Science and Engineering, University of Michigan, Ann Arbor, Michigan 48109-2136

Rare-earth (R) melilite M(R) and its solid solution M′(R) are investigated. Starting with compositions of $R_2Si_3O_3N_4$ and $R_2Si_2AlO_4N_3$, the formation conditions for M(R), M′(R), and their neighboring phases have been delineated, and their lattice parameters and stoichiometry have been determined. Systematic trends in the solubility of M′(R), the unit-cell dimensions, and the competition with neighboring phases with different rare-earth ions have been identified and rationalized in terms of size effects and acid–base reactions. The compatibility between melilite and neighboring phases, including α′- and β′-SiAlON and polytypoids, is summarized in a series of tentative phase diagrams to elucidate the various phase relations for R-Si-(Al/O)-N systems.

I. Introduction

RARE-EARTH-CONTAINING melilite, $R_2Si_3O_3N_4$ (where R is a rare-earth element), is a compound in the R_2O_3–Si_3N_4 binary system. Like akermanite, $Ca_2MgSi_2O_7$, it is a sheet structure with tetragonal symmetry, composed of layers of $Si(O,N)_4$ tetrahedra with large ions such as R^{3+} or Y^{3+} sandwiched in between. This compound, denoted as M(R), is highly refractory and compatible with β-Si_3N_4 and α′-SiAlON. In recent years, evidence also has been accumulated on the formation of an aluminum-containing melilite solid solution M′(R), either as a transient phase during liquid-phase sintering of SiAlON or as a crystallization product during postsintering cooling and annealing.[1–7] This solid solution was identified specifically by Cheng and Thompson[8] in the case of M′(Sm), with a formula of $Sm_2Si_{3-x}Al_xO_{3+x}N_{4-x}$ derived from the systematic substitution of Si—N by Al—O. The terminal substitution of M′(Sm) was estimated to be $x = 1$. This work was extended by Wang *et al.*[9] to M′ solid solutions with R = Nd, Gd, Dy, and Y; they found that the terminal substitution varied from $x = 1$ for R = Nd to $x = 0.6$ for R = Y. Sun *et al.*[10] also found M′ solid solutions to be compatible with α′- and β′-SiAlON in the case of R = Nd and Sm.

Considering the relatively common occurrence of M′(R) in rare-earth-containing SiAlON and its potential use as a sintering-aiding second phase, we have investigated a complete series of rare-earth M(R) and M′(R), for R = even-numbered rare-earth elements, along with their neighboring phases. The compositional ranges of their formation have been delineated, and their phase relations have been elucidated. These results are reported here. In the companion paper,[11] we also have reported several sintered SiAlONs containing M′(R) as a second phase. Their sinterability, mechanical properties, and oxidation resistance are compared to assess their prospect as structural materials.

G. L. Messing—contributing editor

Manuscript No. 192316. Received September 20, 1995; approved February 5, 1996.
Supported by the Air Force Office of Scientific Research under Grant No. AFOSR-F49620-95-1-0119.
Presented at the 96th Annual Meeting of the American Ceramic Society, Indianapolis, IN, April 1994 (Paper No. SXVIIc-137-94).
*Member, American Ceramic Society.

II. Experimental Procedure

Table I provides a nomenclature of various compounds and solid solutions used below, along with the nominal compositions of these phases designated in the starting formulation of our samples. Three main groups of compositions were studied in this work. The first group had a nominal composition of M(R), which was prepared using powder mixtures of rare-earth oxides and silicon nitride. The second group had a nominal composition of M′(R), which was prepared using powder mixtures similar to the above, with additional aluminum oxide. The third group was various M′(R)-SiAlON composites; they were prepared using powder mixtures of rare-earth oxides, aluminum oxide, silicon nitride, and aluminum nitride. The SiAlONs that were investigated included α′, β′, and polytypoid 21R.

Powders used were Si_3N_4 (SN-E10, UBE Industries, Yamaguchi, Japan), AlN (MAN-05, Mitsui Co., Tokyo, Japan), Al_2O_3 (AKP-50, Sumitomo Chemicals, Tokyo, Japan), and various R_2O_3, where R = La, Nd, Sm, Gd, Dy, Er, Yb, and Y (REacton 99.9%, Alfa Products, Wards Hill, MA). We accounted for the surface oxygen content in both Si_3N_4 and AlN powders in the starting formulation. Powders of appropriate proportion were mixed in an agate mortar with isopropyl alcohol. Then, they were dried and pressed into pellets. Either pressureless sintering or hot pressing (HP) was used to effect reaction between 1550° and 1750°C in nitrogen for a period of 1.5–2 h. After reaction, the furnace was turned off and cooling of the sample proceeded at an estimated rate of 37°C/min from 1750° to 1200°C. Annealing at 1550°C for 24 h also was used to crystallize M′(R) in samples that contained only a small amount of melilite.

Reacted samples were polished to remove the material in the outer 0.5 mm on the surface before phase analysis. X-ray diffraction (XRD) using Cu-$K\alpha$ radiation was used for phase identification. To determine the lattice parameters, coarse silicon powders were used as an internal standard. For composition analysis of individual phases, an electron microprobe was used.

III. Results and Discussion

(1) *R-Melilite, M(R)*

Table II gives the results of phase analysis for the nominal composition of $R_2Si_3O_3N_4$ after synthesis. In general, samples in this series were not fully dense, unless HP at temperatures of >1600°C was used. Except for the lanthanum-containing composition, M(R) was always the major phase found. In the case of heavy rare-earth elements—dysprosium, europium, and ytterbium—some J phase ($2R_2O_3 \cdot Si_2N_2O$) also formed; its proportion increased with the atomic number of the rare-earth element. This contrasted with the case of light rare-earth elements, which formed some K phase ($R_2O_3 \cdot Si_2N_2O$) in minority. For lanthanum, only K phase and 1:2 phase ($La_2O_3 \cdot 2Si_3N_4$) were found under all conditions of synthesis. The difficulty of forming M(R) in the case of lanthanum was reported previously by Mitomo *et al.*[12] and confirmed here.

The lattice parameters of M(R) phase vary systematically with the atomic number of rare-earth elements, as shown in Table II. This can be rationalized as a size effect, because the

Table I. Nomenclature

Term	General formula	Compositions designated in starting formulation
α′	$R_xSi_{12-(m+n)}Al_{(m+n)}O_nN_{16-n}$	$R_{0.37}Si_{9.6}Al_{2.4}O_{1.29}N_{14.71}$ ($m = 1.11$, $n = 1.29$, $x = 0.37$)
β′	$Si_{6-x}Al_xO_xN_{8-x}$	$Si_{5.23}Al_{0.77}O_{0.77}N_{7.23}$ ($x = 0.77$ or β_{10})
21R	M_7X_8	$SiAl_6O_2N_6$
12H	M_6X_7	$SiAl_5O_2N_5$
M	$R_2O_3{\cdot}Si_3N_4$	
M′	$R_2Si_{3-x}Al_xO_{3+x}N_{4-x}$	$R_2Si_2AlO_4N_3$ ($x = 1$)
K	$R_2O_3{\cdot}Si_2N_2O$	
J	$2R_2O_3{\cdot}Si_2N_2O$	
J′	$R_4Si_{2-x}Al_xO_{7+x}N_{2-x}$	
1:2	$R_2O_3{\cdot}2Si_3N_4$	
2:1	$2RN{\cdot}Si_3N_4$	
1:1	$R_2O_3{\cdot}AlN$	

ionic radius of rare-earth elements decreases with the atomic number. Figure 1 plots the lattice parameters of M(R) as a function of ionic radius. The unit-cell dimensions increase monotonically with the ionic radius, following a linear relationship.

The tendency for forming different compounds in high-temperature synthesis can be rationalized using the concept of acid–base reactions. This approach recently was applied to reaction densification of α′-SiAlON and found to be capable of explaining such aspects as preferential wetting and formation of transient phases.[6,7] In the present context, we may consider Si_3N_4 as more acidic than Si_2N_2O, which enters the composition of J and K phases, and light rare-earth oxide as more basic than heavy rare-earth oxide. The various minor phases formed in the presence of melilite reaction then can be viewed as the product of the following reactions:

1:2 phase	$La_2O_3{\cdot}2Si_3N_4$	(strong base/strong acid)
K(R) phase	$La_2O_3{\cdot}Si_2N_2O$	(strong base/weak acid)
J(R) phase	$2Yb_2O_3{\cdot}Si_2N_2O$	(weak base/weak acid)

For example, as the basicity of R_2O_3 decreases with decreasing ionic radius, it prefers to react with a weaker acid to form J phase rather than K or 1:2 phase. In the present experiment, because the overall composition was chosen to favor the melilite reaction, these reactions only proceeded to a small extent. It is interesting to note that the molar ratio of base to acid in K(R) and J(R) increases from 1:1 to 2:1; this reflects the need for a larger amount of the weaker base to react with the same acid.

Lastly, we note in Table II that two new (2:1) nitride phases, $Er_2Si_3N_6$ and $Yb_2Si_3N_6$, were found. They are probably isostructural with $Y_2Si_3N_6$,[13] because they all have very similar XRD patterns.

(2) R-Melilite Solid Solution, M′(R)

Table III lists the results of phase analysis for the nominal composition of $R_2Si_2AlO_4N_3$ after synthesis. All of the samples in this series were sintered to high density unless otherwise noted. M′(R) solid solution was found in all cases except ytterbium. Overall, the systematic trend of phase distribution is very similar to that described in the previous section, with the minor phases favoring K phase, in the case of lanthanum, and J phase, in the case of heavy rare-earth elements. The following differences, however, are worth noting.

First, in the case of lanthanum, melilite solid solution formed. This is in contrast to the result obtained for the aluminum-free composition, which did not form La-melilite. The XRD pattern of $La_2Si_2AlO_4N_3$ composition is shown in Fig. 2, in which reflections that can be attributed to the melilite solid solution are labeled. The lattice parameters obtained for these reflections are $a = 7.855$ Å and $c = 5.120$ Å, which are larger than all of the other M(R) and M′(R) found in our study. Using microprobe analysis, the composition of M′(La) was found to be $La_{1.92}Si_{1.82}Al_{0.96}O_{4.21}N_{3.08}$, i.e., essentially an $x = 1$ compound in the $R_2Si_{3-x}Al_xO_{3+x}N_{4-x}$ series.

The results of microprobe analysis, shown in Table IV, also establish the composition of other M′(R) in the series. The x value decreases monotonically with the atomic number of the rare-earth element. This again can be interpreted as a size effect, illustrated by Fig. 3, which plots both the x value and the (cubic root of) unit-cell volume, $(a^2c)^{1/3}$, as a function of ionic radius. Also shown in Fig. 3 is the reference unit-cell volume calculated from Fig. 1, corresponding to $x = 0$. It is clear that the unit cell has expanded in M′(R) relative to M(R). This is accompanied by the substitution of Si—O bond (bond length 1.62 Å) and Si—N bond (1.74 Å) by Al—O bond (1.75 Å).

Table II. Reactions and Phase Formation in $R_2Si_3O_3N_4$ Compositions

Rare-earth element, R	Reaction temperature (°C)/time (h)	Appearance	Phase analysis* by XRD	M(R) lattice parameter (Å)	
				a	*c*
Lanthanum	1650/2 (Sintering)	White	K, 1:2		
	1550/1.5 (HP)	Gray	K, 1:2		
	1600/1.5 (HP)	Gray	K, 1:2		
	1650/1.5 (HP)	Black	1:2, K		
Neodymium	1650/2 (Sintering)	Blue	M, K (vw)	7.721	5.036
	1700/1.5 (HP)	Blue	M, K (w)		
Samarium	1700/2 (Sintering)	White	M, K (vw)		
	1700/1.5 (HP)	Brown	M, K (vw)	7.695	4.991
Gadolinium	1700/2 (Sintering)	White	M, K (vw)	7.650	4.961
Dysprosium	1700/2 (Sintering)	White	M, J (w)	7.618	4.925
Europium	1700/2 (Sintering)	Pink	M, J, 2:1		
	1700/1.5 (HP)	Pink	M, J (mw)	7.585	4.896
Ytterbium	1700/2 (Sintering)	Black	M, J, 2:1		
	1700/1.5 (HP)	Black	M, J (mw)	7.563	4.876

*mw > w > vw.

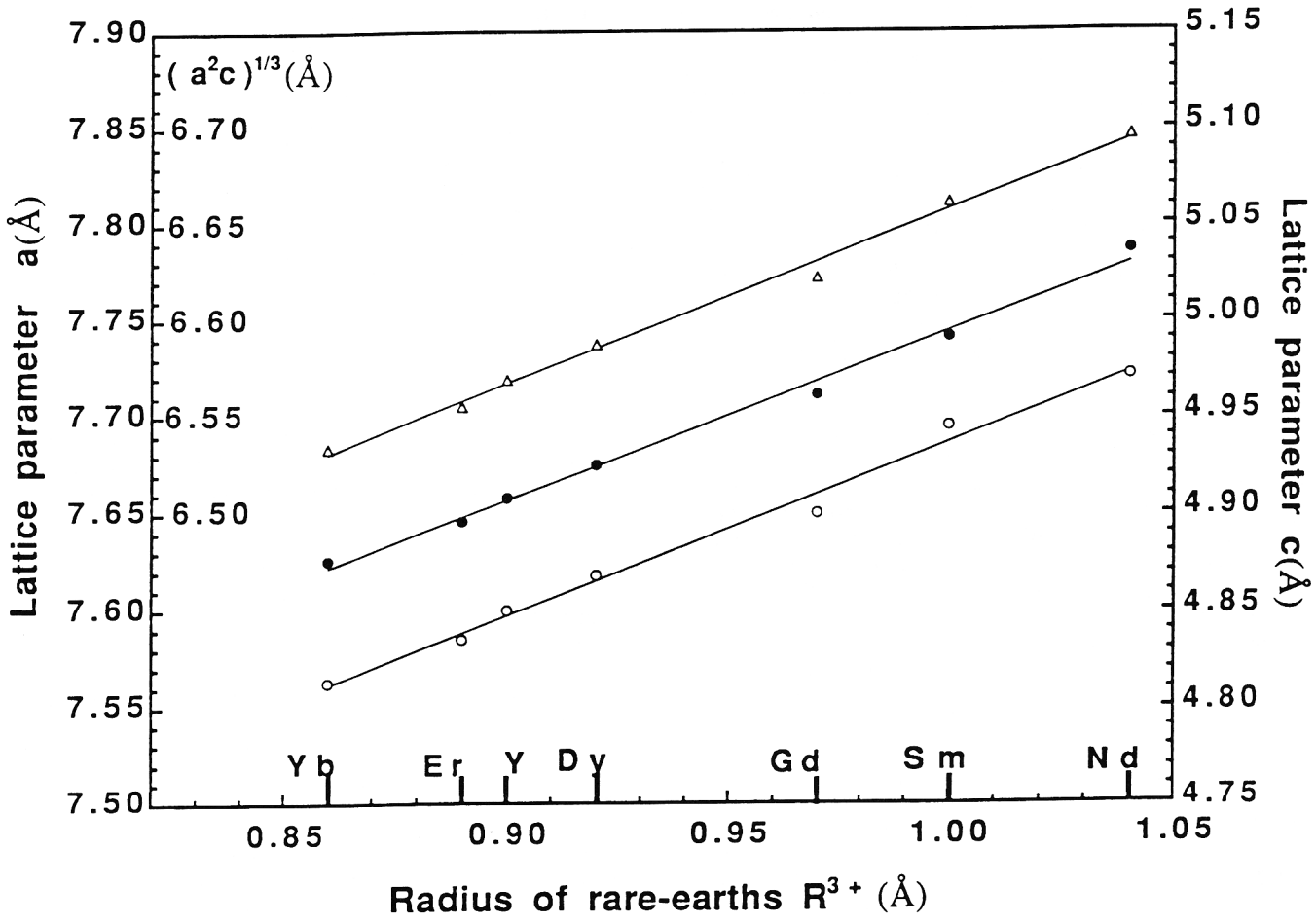

Fig. 1. Lattice parameters of M(R) ((○) *a*, (●) *c*, and (△) $(a^2c)^{1/3}$) as function of ionic radii of rare-earth elements.

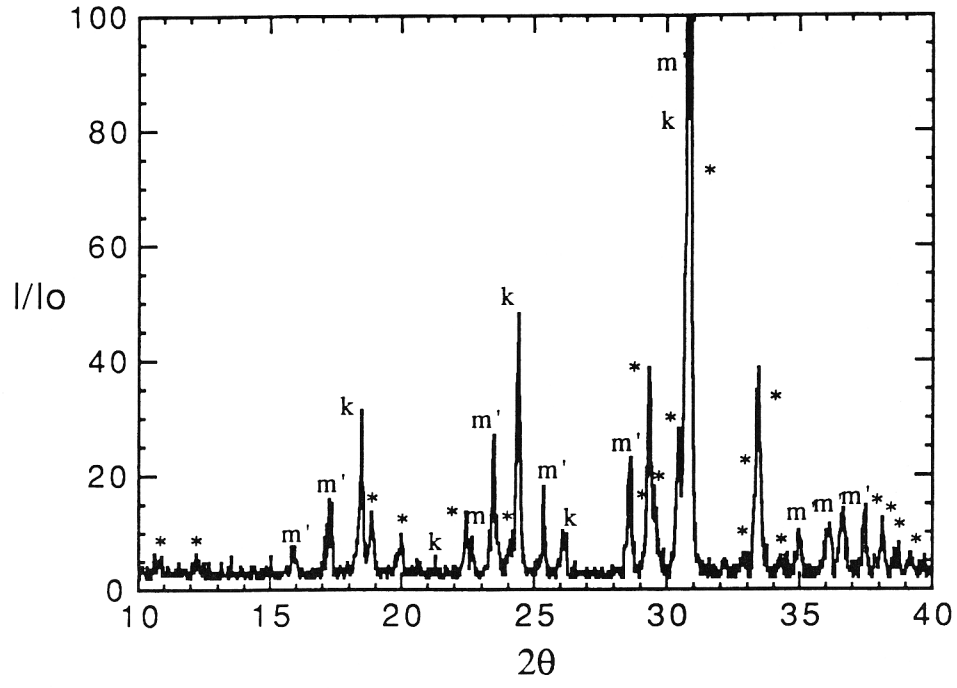

Fig. 2. XRD pattern for $La_2Si_2AlO_4N_3$ composition after heating at 1600°C for 2 h (m′ is M′(La), k is K(La), and * is 1:2).

Table III. Reactions and Phase Formation in $R_2Si_2AlO_4N_3$ Compositions

Rare-earth element, R	Reaction temperature (°C)/time (h)	Appearance	Phase analysis* by XRD	M′(R) lattice parameter (Å)	
				a	*c*
Lanthanum	1650/2	Partly melted	1:2, K		
	1600/2	White, not dense	M′, K, 1:2	7.855	5.120
	1550/1.5 (HP)	Gray	K, 1:2, M′		
Neodymium	1650/2	Purple	M′	7.766	5.055
Samarium	1650/2	Brown	M′	7.730	5.014
Gadolinium	1650/2	Gray	M′	7.689	4.993
Dysprosium	1650/2	Yellow	M′, J′ (vw)	7.655	4.955
Yttrium	1650/2	White	M′, J′ (w)	7.629	4.929
Europium	1650/2	Pink	M′, J′ (mw)	7.608	4.920
Ytterbium†	1650/2	Black	J′		

*mw > w > vw. †Lattice parameters are $a = 7.20$ Å, $b = 10.26$ Å, $c = 10.93$ Å, $\beta = 108.12°$ for all for J′.

Apparently, in the case of lanthanum, which has a very large radius, only after maximal substitution, $x = 1$, is it possible to incorporate lanthanum into the melilite structure. In the case of ytterbium, which has a very small radius in contrast, it is apparently stable only in the limit of smallest volume realizable at $x = 0$. The above values of terminal solubility, x, are consistent with the ones reported by Wang *et al.*[9] for a more-limited series of rare-earth M′ solid solutions.

The lattice parameters of melilite and its solid solution obtained for different rare-earth elements at different x values can be correlated to each other by the following formula:

$$a(\text{Å}) = 6.795 + 0.892r + 0.045x \quad (1)$$

$$c(\text{Å}) = 4.121 + 0.874r + 0.033x \quad (2)$$

where r is the ionic radius (in angstroms) of the rare-earth ion using Ahren's scale. These formulas were obtained by a regression analysis of all the data reported in Tables II and III and can be used for identifying the composition of $R_2Si_{3-x}Al_xO_{3+x}N_{4-x}$ once the identity of the rare-earth element is known. As shown in Fig. 4, which plots the lattice parameter data against the linear combination of r and x given by Eqs. (1) and (2), the agreement between these relations and the data is good.

We now consider the two other phases, K and J, that also were present. Comparing Tables II and III, we note, from neodymium to gadolinium, K phase was present in the aluminum-free composition but not in the aluminum-containing composition. K phase most likely formed by reacting R_2O_3 with surface-oxidized Si_3N_4, forming Si_2N_2O. In the case of the aluminum-containing composition, the oxidized nitride can be incorporated into M′(R) solid solution. Thus, no K phase formed in the latter case. Concerning J phase, our analysis of XRD and microprobe found it also to be a solid solution, J′(R), with a formula of $R_4Si_{2-x}Al_xO_{7+x}N_{2-x}$. The composition of this solid solution was investigated using a microprobe. As shown in Fig. 5, the x value for J′(R) in the $R_2Si_2AlO_4N_3$ reaction increases with the ionic radius of the rare-earth element. This trend is similar to that

Table IV. Microprobe Analysis for $R_2Si_2AlO_4N_3$ Composition after Sintering at 1650°C for 2 h

Phase	Component					Formula
	R	Si	Al	O	N*	
M′(La)						
at.%	16.0	15.2	8.0	35.1	25.7	
Ratio	1.92	1.82	0.96	4.21	3.08	$La_2Si_2AlO_4N_3$†
M′(Nd)						
at.%	17.0	17.9	7.2	32.1	25.8	
Ratio	2.04	2.15	0.86	3.85	3.10	$Nd_2Si_{2.1}Al_{0.9}O_{3.9}N_{3.1}$
M′(Sm)						
at.%	16.5	17.0	7.3	32.1	27.2	
Ratio	1.98	2.04	0.88	3.85	3.26	$Sm_2Si_{2.1}Al_{0.9}O_{3.9}N_{3.1}$
M′(Gd)						
at.%	16.5	17.6	6.3	30.1	29.6	
Ratio	1.98	2.11	0.76	3.61	3.55	$Gd_2Si_{2.2}Al_{0.8}O_{3.8}N_{3.2}$
M′(Dy)						
at.%	17.0	17.5	6.4	31.4	27.7	
Ratio	2.04	2.10	0.77	3.77	3.32	$Dy_2Si_{2.2}Al_{0.8}O_{3.8}N_{3.2}$
J′(Dy)						
at.%	24.0	8.3	4.8	53.5	9.4	
Ratio	3.88	1.34	0.78	7.66	1.34	$Dy_4Si_{1.25}Al_{0.75}O_{7.75}N_{1.25}$
M′(Y)						
at.%	16.3	19.6	5.0	32.7	26.3	
Ratio	1.96	2.36	0.60	3.92	3.16	$Y_2Si_{2.4}Al_{0.6}O_{3.6}N_{3.4}$
J′(Y)						
at.%	25.8	9.2	4.6	52.1	8.2	
Ratio	3.91	1.39	0.70	7.78	1.22	$Y_4Si_{1.3}Al_{0.7}O_{7.7}N_{1.3}$
M′(Er)						
at.%	16.6	19.5	5.2	29.5	29.3	
Ratio	1.99	2.34	0.62	3.54	3.52	$Er_2Si_{2.4}Al_{0.6}O_{3.6}N_{3.4}$
J′(Er)						
at.%	25.3	8.4	4.2	53.3	8.9	
Ratio	4.01	1.33	0.66	7.71	1.29	$Er_4Si_{1.35}Al_{0.65}O_{7.65}N_{1.35}$
J′(Yb)						
at.%	27.7	10.7	3.1	53.8	4.7	
Ratio	4.16	1.61	0.47	8.07	0.70	$Yb_4Si_{1.5}Al_{0.5}O_{7.5}N_{1.5}$

*Deduced from balance. †Sintered at 1600°C for 2 h.

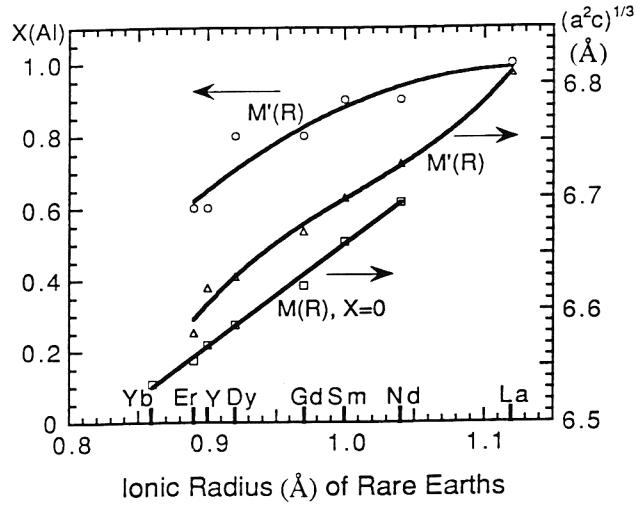

Fig. 3. X(Al) atomic fraction in M′(R) and cell size as function of ionic radii of rare-earth elements.

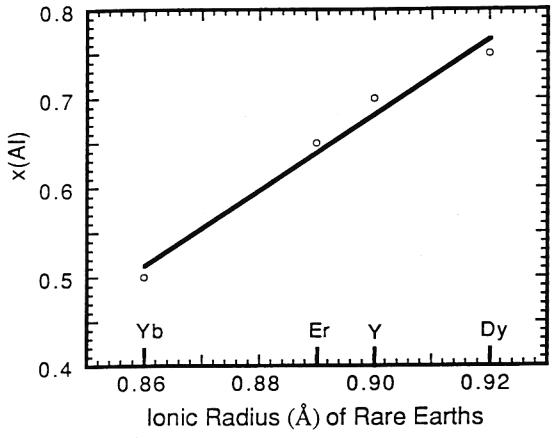

Fig. 5. X(Al) atomic fraction in J′(R) ($R_4Si_{2-x}Al_xO_{7+x}N_{2-x}$) as function of ionic radii of rare-earth elements.

found for M′(R). Although lattice parameters were not determined, considering the relatively low intensity of J′(R) reflections in XRD in $R_2Si_2AlO_4N_3$ compositions, we believe a similar size consideration as that for M′(R) probably holds for these J′(R) phases. Additional tables listing the XRD data of M and M′ solid solutions for various rare-earth elements, as well as J′ solid solution for ytterbium, have been prepared.*

(3) Relations between M′(R) and Neighboring Phases

To elucidate the phase relations between M′(R) and neighboring phases, compositions listed in Table V, using samarium as an example, were investigated. Four three-phase compositions were chosen based on our expectations that they are compatible. Analysis of the resulting phases largely confirmed our expectations, with the following exceptions. First, the composition of α′ found from microprobe analysis was $m = 1.11$ and $n = 0.92$. This composition, representing an apex on the phase boundary of the α′-single-phase region in the α′ plane (i.e., m–n plane), is somewhat different from our original designation of $m = 1.11$ and $n = 1.29$ used in the formulation of the starting three-phase compositions. (The β′ composition, however, coincided with the original designation of β_{10}.) Second, the polytypoid obtained that was compatible with β′ was 12H rather than 21R, as in the original designation, although 21R was compatible with α′, as originally expected. This is reasonable, in retrospect, because the β′ composition is richer in oxygen than α′, thus favoring compatibility with 12H, which also is richer in oxygen than 21R. The above differences were small enough such that the overall composition still remained within the respective three-phase compatibility triangles as originally planned. This is evident from the results of the phase analysis shown in Table V.

Recognizing the systematic trend in M′, J′, α′, and β′ compositions, which vary with different rare-earth elements, a series of tentative diagrams can be drawn to delineate the phase relations between melilite and neighboring phases. (We also have included a rare-earth aluminoxynitride, R_2AlO_3N, denoted as 1:1 in Table V; this phase was found for certain rare-earth elements in our previous study.[14]) Four prototypical diagrams illustrate these relations:

(1) For lanthanum, there is no α′ solid solution; the $x = 1$ compound of M′ forms. In addition, $La_2Si_6O_3N_8$ (1:2 phase) exists as a neighboring phase. These phase relations are illustrated in Fig. 6.

(2) For neodymium and samarium, there is an extensive solid solution of both α′ and M′, but only the J phase, not J′

*Order ACSDD-246 from Data Depository Services, American Ceramic Society, 735 Ceramic Place, Westerville, OH 43081–8720.

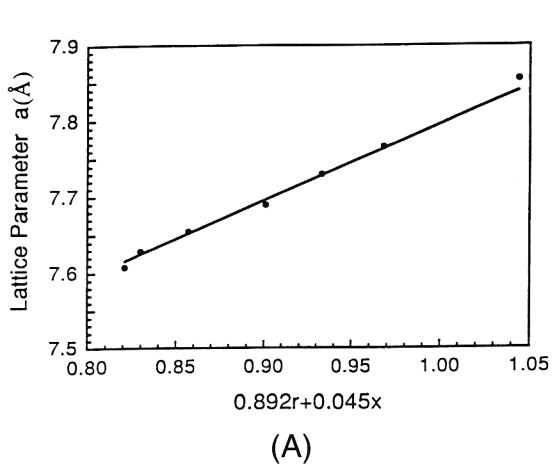

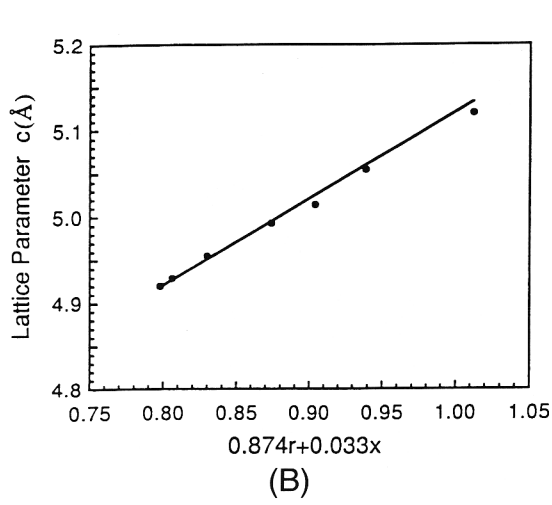

Fig. 4. Comparison of lattice parameters (A) a and (B) c, calculated from Eqs. (1) and (2), respectively, with measured values for each.

Table V. Reactions and Phase Formation in Compositions Containing M′ and Neighboring Phases

Number	Composition (wt%)	Sintering conditions in N_2, temperature (°C)/time (h)	Phase analysis* by XRD
1	80α′:10β′:10M′ (Sm)	1750/2	α′ (vs), β′ (vw), M′ (vw)
		+ 1550/24	α′ (s), β′ (vw), M′ (s)
2	80β′:10α′:10M′ (Sm)	1750/2	β′ (vs), α′ (vw), M′ (vw)
		+ 1550/24	β′ (s), α′ (vw), M′ (s)
3	80α′:10(21R):10M′ (Sm)	1750/2	α′ (vs), 21R (w), M′ (w)
		+ 1550/24	α′ (s), 21R (w), M′ (m)
4	80β′:10(21R):10M′ (Sm)	1750/2	β′ (vs), 12H (w)
		+ 1550/24	β′ (s), 12H (w), M′ (w)
5	76(1:1 (Sm)):24M (Sm)	1550/1.5 (HP)	J (s), M′ (s), 1:1 (mw)
6	76(1:1 (Nd)):24M (Nd)	1550/1.5 (HP)	J (s), M′ (s), 1:1 (m)

*vs > s > m > mw > w > vw.

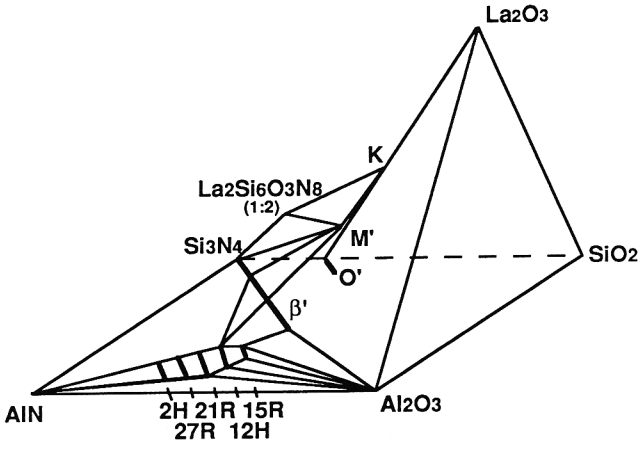

Fig. 6. Phase relations of M′(La) with neighboring phases in La-Si-(Al/O)-N system.

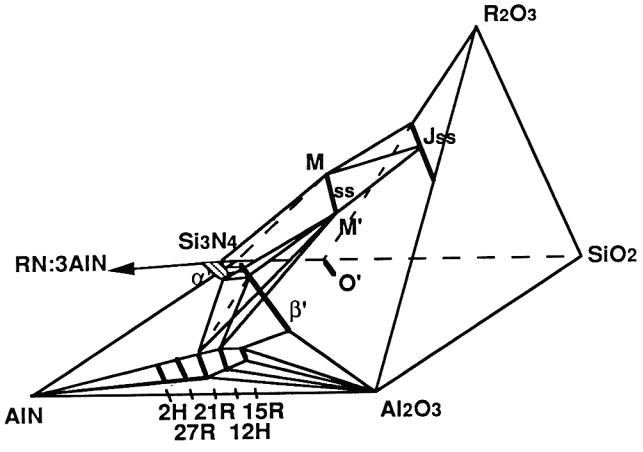

Fig. 8. Phase relations of M′(La) with neighboring phases in R-Si-(Al/O)-N (R = Gd, Dy, Er, Y) system.

solid solution, is compatible with M′. In addition, R_2AlO_3N forms and is compatible with M′ and J. These phase relations are illustrated in Fig. 7. Sun *et al.*[10] also reported that M′ is compatible with $RAlO_3$ (R = Nd, Sm).[10] According to Cheng *et al.*,[5] however, $SmAlO_3$ is stable at temperatures of <1400°C; whereas, M′ is stable between 1400° and 1600°C. Thus, $SmAlO_3$ may not be compatible with M′ but may be just a product that formed during cooling. In the present work, at 1550°C, only coexistence of M′, R_2AlO_3N, and J phase was found.

(3) For gadolinium, dysprosium, europium, and yttrium, there is an extensive solid solution of α′, but the solid-solution range of M′ is somewhat limited. However, J′ solid solution is now compatible with M′, but the compound R_2AlO_3N does not form in this case. These phase relations are illustrated in Fig. 8.

(4) Ytterbium enters α′ solid solution and J′ solid solution. However, only M, not M′, forms in this case. These phase relations are illustrated in Fig. 9.

Additional discussion on the formation of M′ solid solution and the compositional evolution of its neighboring phases dur-

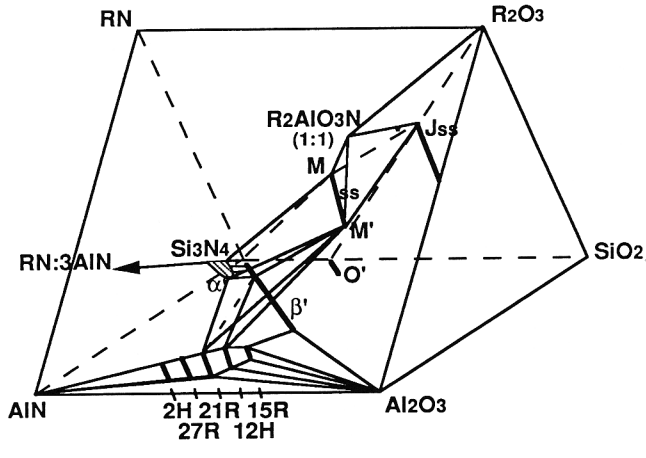

Fig. 7. Phase relations of M′(R) with neighboring phases in R-Si-(Al/O)-N (R = Nd, Sm) system.

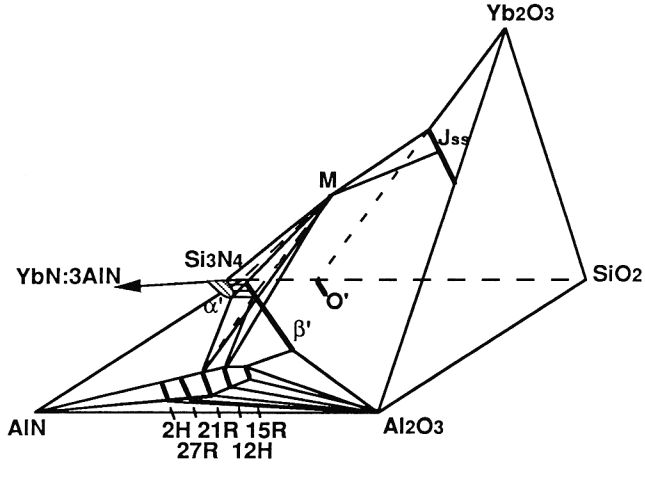

Fig. 9. Phase relations of melilite M(Yb) with neighboring phases in Yb-Si-(Al/O)-N system.

ing low-temperature annealing is postponed to the companion paper.[11]

IV. Conclusions

(1) Melilite $R_2Si_3O_3N_4$ probably exists for all trivalent rare-earth elements except lanthanum; their lattice parameters vary continuously as a function of the ionic size of the rare-earth element.

(2) Melilite solid solution $R_2Si_{3-x}Al_xO_{3+x}N_{4-x}$ probably exists for all trivalent rare-earth elements except ytterbium; their solubility increases as a function of ionic size of the rare-earth element.

(3) Lattice parameters of M′(R) phase have been correlated to an interpolation formula as a function of x and ionic size. J′ solid solution $R_4Si_{2-x}Al_xO_{7+x}N_{2-x}$ probably exists for rare-earth elements from dysprosium to ytterbium; their solubility increases as a function of the ionic size of the rare-earth element.

(4) Formation of competing phases with M(R) and M′(R) involving K, 1:2, 2:1, and J/J′ has been rationalized in terms of acid–base reactions.

(5) Melilite and its solid solutions are compatible with α′- and β′-SiAlON as well as polytypoids. These phase relations involving M/M′ and neighboring phases have been outlined for the R-Si-(Al/O)-N systems.

Acknowledgment: The authors are grateful to Y. B. Cheng for most helpful discussions.

References

[1]P. O. Käll and T. Ekström, "Sialon Ceramics Made with Mixtures of Y_2O_3–Nd_2O_3 as Sintering Aids," *J. Eur. Ceram. Soc.*, **6**, 119–27 (1990).

[2]G. Z. Cao, R. Metselaar, and G. Ziegler, "Formation and Densification of α-Sialon Ceramics"; pp. 1285–93 in *Ceramics Today—Tomorrow's Ceramics*. Edited by P. Vincenzini. Elsevier, Amsterdam, The Netherlands, 1991.

[3]M. Redington and S. Hampshire, "Multi-Cation α-Sialon," *Br. Ceram. Proc.*, **49**, 175–90 (1992).

[4]P. L. Wang, W. Y. Sun, and T. S. Yen, "Sintering and Formation Behavior of R-α-Sialon (R = Nd, Sm, Gd, Dy, Er, and Yb)," *Eur. J. Solid State Inorg. Chem.*, **31** [93] 104 (1994).

[5]Y. B. Cheng and D. P. Thompson, "Preparation and Grain Boundary Devitrification of Samarium α-Sialon Ceramics," *J. Eur. Ceram. Soc.*, **14**, 13–21 (1994).

[6]M. Menon and I-W. Chen, "Reaction Densification of α′-SiAlON: I, Wetting Behavior and Acid–Base Reactions," *J. Am. Ceram. Soc.*, **78** [3] 545–52 (1995).

[7]M. Menon and I-W. Chen, "Reaction Densification of α′-SiAlON: II, Densification Behavior," *J. Am. Ceram. Soc.*, **78** [3] 553–59 (1995).

[8]Y. B. Cheng and D. P. Thompson, "Aluminum-Containing Nitrogen Melilite Phases," *J. Am. Ceram. Soc.*, **77** [1] 143–48 (1994).

[9]P. L. Wang, H. Y. Tu, W. Y. Sun, D. S. Yan, M. Nygren, and T. Ekström, "Study on the Solid Solubility of Al in the Melilite Systems $R_2Si_{3-x}Al_xO_{3+x}N_{4-x}$ with R = Nd, Sm, Gd, Dy and Y," *J. Eur. Ceram. Soc.*, **15**, 689–93 (1995).

[10]W. Y. Sun, D. S. Yan, L. Gao, H. Mandal, K. Liddell, and D. P. Thompson, "Subsolidus Phase Relationships in the Systems Ln_2O_3–Si_3N_4–AlN–Al_2O_3 (Ln=Nd, Sm)," *J. Eur. Ceram. Soc.*, **15**, 349–55 (1995).

[11]Z.-K. Huang, S.-Y. Liu, A. Rosenflanz, and I-W. Chen, "SiAlON Composites Containing Rare-Earth Melilite and Neighboring Phases," *J. Am. Ceram. Soc.*, **79** [8] 2081–90 (1996).

[12]M. Mitomo, F. Izumi, S. Horiuchi, and Y. Matsui, "Phase Relationships in the System Si_3N_4–SiO_2–La_2O_3," *J. Mater. Sci.*, **17**, 2359–64 (1982).

[13]W. Y. Sun, T. Y. Tien, and T. S. Yen, "Subsolidus Phase Relationships in Part of the System Si,Al,Y/N,O," *J. Am. Ceram. Soc.*, **74** [11] 2753–58 (1991).

[14]Z.-K. Huang, D. S. Yan, and T. Y. Tien, "Compound Formation and Melting Behavior in the AB Compound and Rare Earth Oxide System," *J. Solid State Chem.*, **85**, 51–55 (1990). □